

Major perturbation of ocean chemistry and a 'Strangelove Ocean' after the end-Permian mass extinction

Michael R. Rampino^{1,2} and Ken Caldeira³

¹Earth and Environmental Science Program, New York University, 100 Washington Square East, New York, NY 10003, USA;

²Goddard Institute for Space Studies, NASA, New York, NY 10025, USA; ³Department of Global Ecology, Carnegie Institution, 200 Panama St., Stanford, CA 94305, USA

ABSTRACT

The severe mass extinction of marine and terrestrial organisms at the end of the Permian Period (c. 251 Ma) was accompanied by a rapid (<100 000 years and possibly <10 000 years) negative excursion of c. 3‰ in the $\delta^{13}\text{C}$ of the global surface oceans and atmosphere that persisted for some 500 000 years into the Early Triassic. Simulations with an ocean–atmosphere/carbon-cycle model suggest that the isotope excursion can be explained by collapse of ocean primary productivity, and changes in the delivery and cycling of carbon in the oceans and on land. Model results suggest that severe reduction of

marine productivity led to an increase in surface-ocean dissolved inorganic carbon and a rapid, short-term increase in atmospheric pCO_2 (from a Late Permian base of 850 ppm to c. 2500 ppm). Increase in surface ocean alkalinity may have stimulated the widespread microbial and abiotic shallow-water carbonate deposition seen in the earliest Triassic. The model is also consistent with a long-term (>1 Ma) decrease in sedimentary burial of organic carbon in the early Triassic.

Terra Nova, 17, 554–559, 2005

Introduction

The mass extinction of marine and terrestrial organisms at the end of the Permian Period (c. 251 Ma) was the most severe known in the geological record (Erwin, 1993). The extinction was accompanied by a rapid negative shift of c. 3‰ in the $\delta^{13}\text{C}$ of the global surface oceans and atmosphere (Magaritz *et al.*, 1992; Wang *et al.*, 1995; MacLeod *et al.*, 2000). An important clue to the cause of the negative isotope excursion and the eventual recovery of life in the Triassic Period is the pace of the shift. Causes that involve changes in the balance of buried and eroded carbon and/or changes in weathering rates involve the carbonate/silicate rock weathering cycle, with a long time scale on the order of hundreds of thousands to millions of years (Bernier, 1994; Bernier and Kothala, 2001). On the contrary, causes that involve variations in the distribution of carbon and carbon isotopes within the ocean–atmosphere system, such as a collapse of marine productivity (Kump and Arthur, 1999; Bernier, 2002; Zeebe and Westbroek,

2003) occur on a shorter timescale of thousands to tens of thousands of years.

Precise radiometric dating was used to constrain the end-Permian extinction pulse in China within an interval of <1 million years, and the negative carbon-isotope shift to less than c. 165 000 years (Bowring *et al.*, 1998). Using the improved resolution provided by Milankovitch cyclostratigraphic analysis across the Permian–Triassic (P–Tr) boundary in the Austrian Alps, Rampino *et al.* (2000) estimated that the abrupt marine faunal change could have occurred in ≤ 8000 years. The initial negative carbon-isotope shift is estimated to have occurred rapidly within an interval of ≤ 30 000 years coincident with the extinctions, and the longer-term transient negative carbon-isotope excursion lasted c. 500,000 years into the Early Triassic.

In the oceans, shallow-water calcareous organisms (e.g. corals, brachiopods, foraminifera, crinoids) suffered drastic extinctions and planktonic organisms (e.g. radiolarians) were also apparently hard hit (Wignall and Newton, 2003). On land, vertebrates and insects suffered a major extinction (Erwin, 1993; Smith and Ward, 2001), and most Late Permian gymnosperm palynomorphs and plant macrofossils disappeared at a level marked by a flood of fungal spores (Visscher *et al.*, 1996). In fact, coal deposits are

unknown in Lower Triassic strata, and recovery of plant diversity apparently took c. 4 million years (Retallack *et al.*, 1996; Visscher *et al.*, 1996; Looy *et al.*, 1999). These changes, along with an increase in land-derived organic material in marine sediments, suggest a major perturbation of the carbon cycle on land at the end of the Permian (Visscher *et al.*, 1996).

Model simulation of carbon-isotope excursion

In order to investigate the possibility that the rapid decrease in $\delta^{13}\text{C}$ was caused primarily by a change in ocean–atmosphere carbon distribution brought about by the marine and non-marine extinctions and productivity collapse, we performed simulations using a geochemical model of the carbon cycle, which considers interactions among Earth's ocean, atmosphere and rock reservoirs (for details of the model, see Caldeira and Rampino, 1993).

The ocean–atmosphere component of the model is based on a 3-box ocean plus atmosphere model of Toggweiler and Sarmiento (1985). Treatment of carbon-isotopic fractionation follows that of Zhang *et al.* (1995). Representation of shallow-water carbonate deposition in the model follows that of Opdyke and Wilkinson (1993), where shallow-water carbonate production (F_{sw}) is

Correspondence: Dr Michael R Rampino, Earth and Environmental Science Program, New York University, 100 Washington Square East, Room 1009, New York, NY 10003, USA. Tel.: 001 212 998 3743; fax: 001 212 995 4015; e-mail: mrr1@nyu.edu

a function of surface-ocean carbonate-ion concentration:

$$F_{sw} = k(\Omega - 1)^\eta$$

where Ω is the saturation state for calcium carbonate, k is a rate constant and η is the order of reaction, which is estimated as about 1.7–2 (Caldeira and Rampino, 1993; Opdyke and Wilkinson, 1993; Zeebe and Westbroek, 2003).

Geological evidence indicates that pelagic carbonate production was essentially zero prior to the appearance of calcareous plankton in the Jurassic Period (Berner, 1994), the typical 'Neritan Ocean' of Zeebe and Westbroek (2003). Partly a result of the lack of pelagic carbonate deposition, and thus higher alkalinity and carbonate-ion concentrations in the oceans, our model predicts that the Late Permian oceans contained about twice the amount of dissolved inorganic carbon as recent oceans.

The ocean–atmosphere model is embedded within a representation of the long-term geochemical carbon cycle based on the GEOCARB II and III models of Berner (1994) and Berner and Kothala (2001). We adjusted the model for estimated Late Permian conditions by using a volcanic release rate for CO_2 that is *c.* 10% greater than at present (as in the GEOCARB models under steady-state conditions silicate-rock weathering balances volcanic CO_2 release). We also used a Late Permian land area vs. ocean area ratio *c.* 90% of the present ratio, leading to predicted Late Permian atmospheric pCO_2 levels about three times pre-industrial pCO_2 or *c.* 850 ppm (Berner, 1994). To calculate global temperature change with change in atmospheric pCO_2 we use the parameterization of Berner (1994). Estimates of climate sensitivity (including the effects of reduced solar output in the past) suggest a Late Permian global climate *c.* 1 °C warmer than present.

In order to test whether a drastic decrease in ocean productivity and biomass at the end of the Permian could have produced the observed carbon-isotope record, the model was run in a time-dependent mode, in which marine surface productivity was abruptly set to zero. We also introduced a long-term 15% reduction in the fraction of carbon buried as

organic carbon in an attempt to account for a longer-term shift in the steady-state of $\delta^{13}\text{C}$ in marine carbonates (Broecker and Peacock, 1999; Kump and Arthur, 1999; Berner, 2002). In this simulation, we allowed biological productivity to return to pre-cessation levels exponentially (more rapidly at first) on a 1 million-year time scale.

Model results

Model results for atmospheric carbon dioxide and marine carbonate sedimentation are presented in Fig. 1. The cessation of marine biological export of organic carbon from the surface ocean leads to an increase in surface-ocean dissolved inorganic carbon concentration, some of which leaks into the atmosphere to increase atmospheric pCO_2 (Fig. 1). However, this

addition of carbon to the surface ocean also diminishes the carbonate ion concentration of surface waters. This, in turn, reduces the rate of alkalinity removal in shallow-water carbonates because carbonate deposition rates in shallow-water environments apparently depend on the degree of oceanic super-saturation (Opdyke and Wilkinson, 1993; Gattuso *et al.*, 1998; Kleypas *et al.*, 1999; Langdon *et al.*, 2000).

Alkalinity would then build up in the ocean as a result of the combined effects of enhanced riverine alkalinity (from increased weathering rates) and a diminished shallow-water alkalinity sink (Caldeira and Rampino, 1993). This buildup in alkalinity draws CO_2 back into the ocean from the atmosphere. Hence, the time scale for recovery of atmospheric pCO_2 is governed by the time scale of equilibrium of

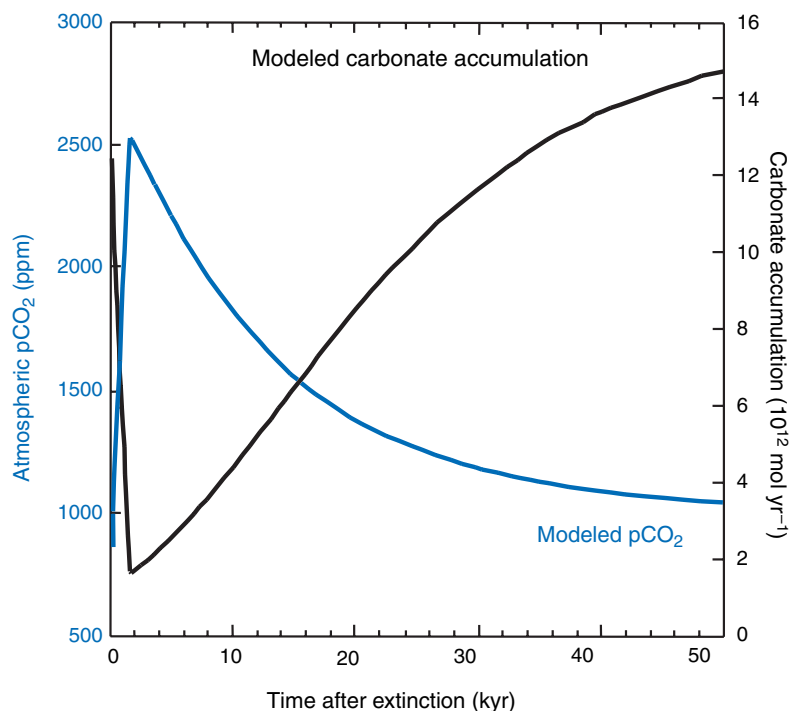


Fig. 1 Results of model simulation for shallow-water carbonate accumulation rates (mol year^{-1}) (black) and atmospheric pCO_2 (ppm) (blue) for the first 50 000 years after a sudden ocean productivity collapse. Atmospheric and surface ocean carbon dioxide initially increase as a result of a cessation of biological carbon transport from the surface to the deep ocean. This increase in surface-ocean carbon diminishes carbonate mineral super-saturation of the surface ocean and thus decreases shallow-water carbonate accumulation. Because alkalinity continues to be transported to the ocean from continental weathering, there is a net flux of alkalinity to the oceans that draws most of the CO_2 increase back into the ocean on the roughly 10^4 year timescale of the carbonate system.

ocean chemistry with the carbonate system (*c.* 10^4 years) (Archer *et al.*, 1997). Increased ocean alkalinity may have had the added effect of further lowering the $\delta^{13}\text{C}$ of marine carbonates (Riding, 1997). Beyond the first 50 000 years shown in Fig. 1, the atmospheric pCO_2 level continues to recover on the slower time scale of the carbonate/silicate cycle (Berner, 1994), and carbonate sedimentation returns to a balance with chemical weathering. After about a million years, the system has effectively reached a new steady-state, and atmospheric pCO_2 levels no longer change appreciably.

In our model, when ocean productivity is turned off, atmospheric pCO_2 rises by *c.* 1700 ppm, whereas a cessation of productivity today would result in only about a doubling of atmospheric pCO_2 , or an increase of *c.* 300 ppm. The main reason for this difference is that the P-Tr shift in surface-ocean $\delta^{13}\text{C}$ of *c.* -3‰ suggests that the surface-to-deep $\delta^{13}\text{C}$ gradient in the Late Permian oceans was significantly greater than today's surface-to-deep $\delta^{13}\text{C}$ difference. Therefore, the pre-P-Tr extinction ocean would have had greater biological carbon export relative to ocean mixing than exists in the modern ocean. Thus, when the biological carbon export is turned off, the rise in atmospheric pCO_2 is proportionately greater.

Model results suggest that the oceans could have maintained an approximate balance between sedimentation and the weathering fluxes of carbon and alkalinity although marine productivity of carbonate and organic carbon were sharply reduced in the earliest Triassic. This continued near-balance could have been the result of an increase in shallow-water abiotic and microbial carbonate deposition as a direct response to increased surface-water carbonate-ion concentrations (Caldeira and Rampino, 1993; Opdyke and Wilkinson, 1993). Studies of open-shelf and platform P-Tr boundary sections show evidence for an Early Triassic increase in inorganic carbonate accumulation in the form of oolites, carbonate cements, and sea-floor carbonate precipitation. Microbialite and algal carbonate crusts are also widespread in shallow-water settings in the earliest Triassic (e.g. Reinhardt, 1988; Schubert and Bottjer, 1992; Baud *et al.*,

1997; Sano and Nakashima, 1997; Kershaw *et al.*, 1999; Lehrmann *et al.*, 2003), and it is known that microbial calcification responds primarily to the supply of bicarbonate (Riding, 1997)]. Our results indicate that this mechanism of inorganic and algal/microbial deposition of CaCO_3 might have prevented an "alkalinity crisis" during which the deep oceans could have become fully saturated with respect to calcite (Caldeira and Rampino, 1993). In deeper shelf sections, such as Meishan in China, calculated sediment accumulation rates dropped precipitously in the transitional P-Tr beds, but then rose again in Lower Triassic strata (Bowring *et al.*, 1998).

Carbon isotopes provide a proxy for fluctuations of marine productivity and burial rates of organic carbon (Kump and Arthur, 1999; Berner, 2002). Model results for carbon-isotope changes in the surface ocean are shown in Fig. 2. In the initial 1000 years after the collapse of marine productivity in the model, the carbon-isotope value of the surface-ocean mixed layer drops precipitously and becomes as light as that of the deep ocean – the Strangelove Ocean effect (e.g. Kump and Arthur, 1999; Berner, 2002). During the subsequent 500 000 years, surface-ocean $\delta^{13}\text{C}$ recovers toward pre-perturbation levels. Atmospheric $\delta^{13}\text{C}$ in the model follows the surface-ocean values.

We compared our surface-ocean carbon-isotope model results with the carbon-isotope data for the GK-1 core (Austria) (Magaritz and Holser, 1991; Magaritz *et al.*, 1992) (Fig. 2a), where previous work on Milankovitch-scale cycles in the core allow us to estimate sedimentation rates, and hence time in the core record (Rampino *et al.*, 2000). The carbon-isotopic record at the end of the Permian is consistent with our simulation of a rapid collapse of ocean productivity (Kump and Arthur, 1999). The *c.* 3‰ magnitude of the shift agrees with estimates of Late Permian ocean-carbon content, and the time scale of isotopic recovery in the oceans of *c.* 500 000 years (Magaritz and Holser, 1991) is similar to that seen for carbon isotopes in the model simulation. The rapid isotope shift is indicative of a collapse in marine production, and is too rapid to be explained solely by a net reduction in the organic carbon burial rate.

The $\delta^{13}\text{C}$ curve in the GK-1 core shows an additional negative excursion *c.* 300 000–400 000 years after the initial negative $\delta^{13}\text{C}$ shift (Fig. 2b). This may be a global effect, revealed by the high resolution of the GK-1 section, or it may represent conditions unique to the Gartnerkofel locality (Magaritz and Holser, 1991). The subsequent negative shift in $\delta^{13}\text{C}$ suggests a second productivity crash, but we discovered that we could not simulate the negative excursion solely by decreasing productivity. The reason appears to be that ocean-surface productivity had not recovered sufficiently by 300 000 years after the initial crash in the model to allow a second crash to decrease productivity sufficiently to produce the required -1.5‰ shift in $\delta^{13}\text{C}$.

Therefore, in order to simulate the second negative $\delta^{13}\text{C}$ shift, we had to also decrease net organic carbon burial in our model by 1% for each 10% reduction in biological productivity (Fig. 2b). Marine biological productivity was allowed to increase linearly from zero to 50% of the Late Permian productivity in the 200 000 years after the initial $\delta^{13}\text{C}$ shift, with a linear collapse to zero productivity in the subsequent 200 000 years. This was followed by an exponential recovery to full production with a time constant of *c.* 100 000 years.

The long-term (*c.* 10^6 year) shift in carbon-isotope ratio across the P-Tr boundary cannot be explained by ocean/atmosphere reservoir effects, but must involve a decrease in the ratio of burial of organic carbon to CaCO_3 (Broecker and Peacock, 1999; Berner, 2002). The end-Permian extinction apparently led to a situation where the accumulation of organic matter in the sea dominated over accumulation of organic debris on land (Broecker and Peacock, 1999). The severe plant extinction apparently devastated the complex ecosystems responsible for massive continental carbon storage (Retallack *et al.*, 1996; Visscher *et al.*, 1996; Michaelsen, 2002). At the same time, the loss of an efficient marine food web may have led to enhanced preservation of organic matter falling through the water column (D'Hondt *et al.*, 1998).

Oxygen-isotope data from the GK-1 core (Magaritz and Holser, 1991)

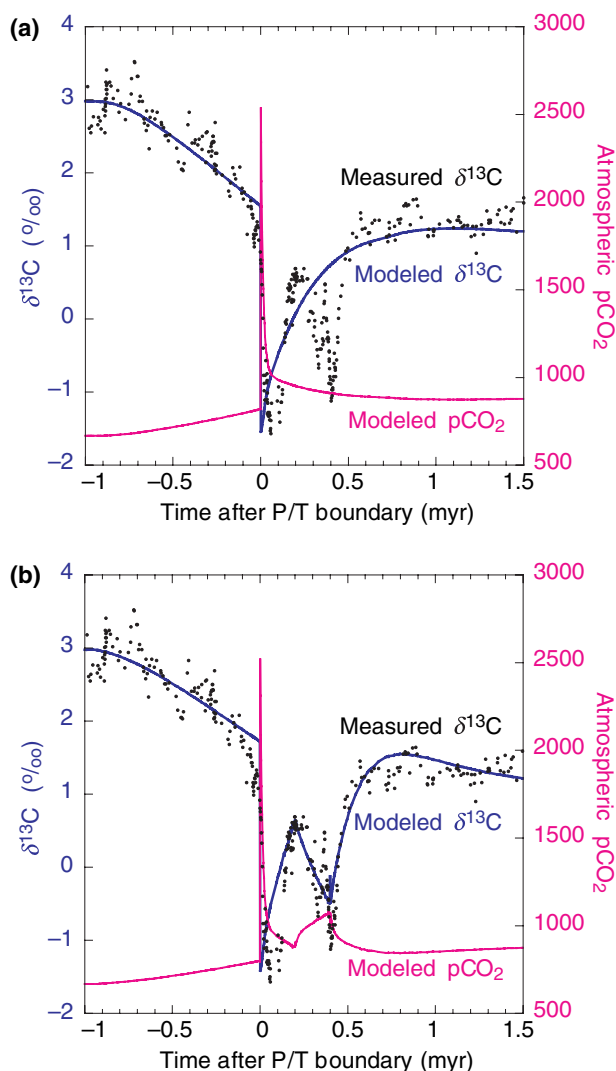


Fig. 2 (a) Results of model simulation for $\delta^{13}\text{C}$ of ocean-surface waters (blue) compared with $\delta^{13}\text{C}$ data from the GK-1 core from the Carnic Alps, Austria (black dots) (Magaritz and Holser, 1991). In this case, the second $\delta^{13}\text{C}$ shift at *c.* 300 ka after the extinction event is interpreted as a local signal. (b) Results of model simulation considering that the $\delta^{13}\text{C}$ shift at of ocean-surface waters *c.* 300 ka after the extinction event represents a global signal. This model run includes partial recovery of marine productivity followed by a second collapse in productivity, and a reduction in the rate of burial of organic carbon (see text). The long-term shift in model surface-water $\delta^{13}\text{C}$ from late Permian to Early Triassic was simulated by a 15% decrease in organic carbon burial. Also plotted is the predicted perturbation of atmospheric pCO₂ (red) calculated by the model. Time scale for the GK-1 core is after the cyclostratigraphy of Rampino *et al.* (2000).

suggest that a significant climate warming of $> 6^\circ\text{C}$ may have occurred during earliest Triassic time. Study of leaf stomatal density in earliest Triassic (Griesbachian) plants suggests an elevated atmospheric pCO₂ content of > 2000 ppm (Retallack, 2001) in agreement with our model results (Fig. 1). The resultant tripling of atmospheric pCO₂ in the earliest

Triassic (Fig. 2) is estimated to have produced *c.* 6°C of global warming over Late Permian climate.

Discussion and conclusions

Model results suggest that collapse of ocean productivity (Strangelove Ocean) accompanying the end-Permian mass extinction could have

been the primary cause of the rapid negative shift of *c.* 3 per mil in the $\delta^{13}\text{C}$ of global open ocean-surface waters at that time. The transient $\delta^{13}\text{C}$ change persisted for *c.* 500 000 years into the Early Triassic. The Strangelove Ocean scenario would be determination of the $\delta^{13}\text{C}$ content of carbonate deposited in benthic environments in the deep ocean. For a Strangelove Ocean, deep benthic $\delta^{13}\text{C}$ should not change significantly across the end-Permian extinction interval (e.g., Kump and Arthur, 1999). For an alternative cause of the isotope shift by rapid addition of light carbon to the entire ocean/atmosphere system (e.g. methane-hydrate release), deep benthic carbonate should show a significant $\delta^{13}\text{C}$ decrease mirroring that of surface waters and the atmosphere.

The model also predicts a transient increase in atmospheric pCO₂ of short duration (< 50 000 years) compared with the perturbation of carbon-isotope ratios (several hundred thousand years). This is explained by the fact that the rate of recovery of atmospheric pCO₂ to pre-perturbation levels is governed by chemical equilibration between atmosphere, ocean and sediments, whereas the rate of recovery of $\delta^{13}\text{C}$ depends upon the much slower exchange of carbon in the ocean and atmosphere with carbon in the rock reservoir (Caldeira and Rampino, 1993; Berner, 1994).

Ocean-surface $\delta^{13}\text{C}$ in the Early Triassic recovered to values *c.* 1 or 2‰ lower than those of the Late Permian (Fig. 2), which could have been a consequence of a long-term reduction in the fraction of carbon buried as organic carbon resulting from a shift in the major locus of carbon burial from the continents to the ocean basins (Broecker and Peacock, 1999; Berner, 2002). This reduction in global organic carbon burial on land was most likely the direct result of the mass extinction of land plants and their extended period of recovery (Michaelsen, 2002).

Our model results for times of productivity collapse at the end of the Permian agree with geological evidence for rapid negative shifts in $\delta^{13}\text{C}$, brief global warming, initial reduction in calcium carbonate depos-

ition, and enhanced deposition of shallow-water abiotic (?) and microbial (cyanobacterial) carbonates. The rapid, transient negative carbon-isotope shifts in ocean waters and the atmosphere make a good correlation tool between marine and non-marine sections, and provides a global chemostratigraphic marker for the P-Tr extinction event (Twitchett *et al.*, 2001).

Acknowledgements

We thank R. Berner, W.S. Broecker, C. Koeberl, E. Krull, T. Volk and P. Wignall for reviews. The study was supported in part by a New York University Research Challenge Grant.

References

- Archer, D., Kheshgi, H. and Maier-Reimer, E., 1997. Multiple timescales for neutralization of fossil fuel CO₂. *Geophys. Res. Lett.*, **24**, 405–408.
- Baud, A., Cirilli, S. and Marcoux, J., 1997. Biotic response to mass extinction: the lowermost Triassic microbialites. *Facies*, **36**, 238–242.
- Berner, R.A., 1994. GEOCARB II: a revised model of atmospheric CO₂ over Phanerozoic time. *Am. J. Sci.*, **294**, 56–91.
- Berner, R.A., 2002. Examination of hypothesis for the Permo-Triassic boundary extinction by carbon cycle modeling. *Proc. Natl Acad. Sci. USA*, **99**, 4172–4177.
- Berner, R.A. and Kothala, Z., 2001. GEOCARB III: a revised model of atmospheric CO₂ over Phanerozoic time. *Am. J. Sci.*, **301**, 182–204.
- Bowring, S.A., Erwin, D.H., Jin, Y.G., Martin, M.W., Davidek, K. and Wang, W., 1998. U/Pb zircon geochronology and tempo of the end-Permian mass extinction. *Science*, **280**, 1039–1045.
- Broecker, W. S. and Peacock, S., 1999. An ecologic explanation for the Permian-Triassic carbon and sulfur isotope shifts. *Global Biogeochem. Cycles*, **13**, 1167–1172.
- Caldeira, K. and Rampino, M.R., 1993. The aftermath of the K/T boundary mass extinction: biogeochemical stabilization of the carbon cycle and climate. *Paleoceanography*, **8**, 515–525.
- D'Hondt, S., Donaghay, P., Zachos, J.C., Luttenberg, D. and Lindlinger, M., 1998. Organic carbon fluxes and ecological recovery from the Cretaceous-Tertiary mass extinction. *Science*, **282**, 276–279.
- Erwin, D.H., 1993. *The Great Paleozoic Crisis*. Columbia University Press, New York.
- Gattuso, J.-P., Frankignoulle, M., Bourge, I., Romaine, S.W. and Buddemeier, R.W., 1998. Effect of calcium carbonate saturation of seawater on coral calcification. *Global Planet. Change*, **18**, 37–46.
- Kershaw, S., Zhang, T. and Lan, G., 1999. A ?microbialite carbonate crust at the Permian-Triassic boundary in South China, and its palaeoenvironmental significance. *Palaeogeogr. Palaeoclimatol. Palaeoecol.*, **146**, 1–18.
- Kleypas, J.A., Buddemeier, R.W., Archer, D., Gattuso, J.-P., Langdon, C. and Opdyke, B.N., 1999. Geochemical consequences of increased atmospheric carbon dioxide on coral reefs. *Science*, **284**, 118–120.
- Kump, L.R. and Arthur, M.A., 1999. Interpreting carbon-isotope excursions: carbonates and organic matter. *Chem. Geol.*, **161**, 181–198.
- Langdon, C., Takahashi, T., Sweeney, C., Chipman, D., Goddard, J., Marubini, F., Aceves, H., Barnett, H. and Atkinson, M.J., 2000. Effect of calcium carbonate saturation state on the calcification rate of an experimental coral reef. *Global Biogeochem. Cycles*, **14**, 639–654.
- Lehrmann, D.J., Payne, J.L., Felix, S.V., Dillett, P.M., Wang, H., Yu, Y. and Wei, J., 2003. Permian-Triassic boundary sections from shallow-marine carbonate platforms of the Nanpanjiang Basin, South China: implications for oceanic conditions associated with the end-Permian extinction and its aftermath. *Palaios*, **18**, 138–152.
- Looy, C.V., Brugman, W. A., Dilcher, D.L. and Visscher, H., 1999. The delayed resurgence of equatorial forests after the Permian-Triassic ecologic crisis. *Proc. Natl Acad. Sci. USA*, **96**, 13857–13862.
- MacLeod, K.G., Smith, R.M.H., Koch, P.L. and Ward, P.D., 2000. Timing of mammal-like reptile extinctions across the Permian-Triassic boundary in South Africa. *Geology*, **28**, 227–230.
- Magaritz, M. and Holser, W.T., 1991. The Permian-Triassic of the Gartnerkofel-I core (Carnic Alps, Austria): carbon and oxygen isotope variation. *Abh. Geol. Bundesanst.*, **45**, 149–163.
- Magaritz, M., Krishnamurthy, R.V. and Holser, W.T., 1992. Parallel trends in organic and inorganic carbon isotopes across the Permian-Triassic boundary. *Am. J. Sci.*, **292**, 727–739.
- Michaelsen, P., 2002. Mass extinction of peat-forming plants and the effect on fluvial styles across the Permian-Triassic boundary, northern Bowen Basin, Australia. *Palaeogeogr. Palaeoclimatol. Palaeoecol.*, **179**, 173–188.
- Opdyke, B.N. and Wilkinson, B. H., 1993. Carbonate mineral saturation state and cratonic limestone accumulation. *Am. J. Sci.*, **293**, 217–234.
- Rampino, M.R., Prokoph, A. and Adler, A.C., 2000. Tempo of the end-Permian event: high-resolution cyclostratigraphy at the Permian-Triassic boundary. *Geology*, **28**, 643–646.
- Reinhardt, J.W., 1988. Uppermost Permian reefs and Permo-Triassic sedimentary facies from the southeastern margin of Sichuan Basin, China. *Facies*, **18**, 231–288.
- Retallack, G.J., 2001. A 300-million-year record of atmospheric carbon dioxide from fossil plant cuticles. *Science*, **411**, 287–290.
- Retallack, G.J., Veevers, J.J. and Morante, R., 1996. Global coal gap between Permian-Triassic extinction and Middle Triassic recovery of peat-forming plants. *Geol. Soc. Am. Bull.*, **108**, 195–207.
- Riding, R., 1997. Stromatolite decline: a brief reassessment. *Facies*, **36**, 227–230.
- Sano, H. and Nakashima, K., 1997. Lowermost Triassic (Griesbachian) microbial bindstone-cementstone facies, southwest Japan. *Facies*, **36**, 1–24.
- Schubert, J.K. and Bottjer, D.J., 1992. Early Triassic stromatolites as post-mass extinction disaster forms. *Geology*, **20**, 883–886.
- Smith, R.M.H. and Ward, P.D., 2001. Pattern of vertebrate extinctions across an event bed at the Permian-Triassic boundary in the Karoo Basin of South Africa. *Geology*, **29**, 1147–1150.
- Toggweiler, J.R. and Sarmiento, J.L., 1985. Glacial to interglacial changes in atmospheric carbon dioxide: the critical role of ocean surface water in high latitudes. *Geophys. Monogr.*, **25**, 163–184.
- Twitchett, R.J., Looy, C., Morante, R., Visscher, H. and Wignall, P.B., 2001. Rapid and synchronous collapse of marine and terrestrial ecosystems during the end-Permian biotic crisis. *Geology*, **29**, 351–354.
- Visscher, H., Brinkhuis, H., Dilcher, D.L., Elsik, W.C., Eshet, Y., Looy, C.V., Rampino, M.R. and Traverse, A., 1996. The terminal Paleozoic fungal event: evidence of terrestrial ecosystem destabilization and collapse. *Proc. Natl Acad. Sci. USA*, **93**, 2155–2158.
- Wang, K., Geldsetzer, H.H.J. and Krouse, H. R., 1995. Permian-Triassic extinction: Organic $\delta^{13}\text{C}$ evidence from British Columbia, Canada. *Geology*, **22**, 580–584.
- Wignall, P.B. and Newton, R., 2003. Contrasting deep-water records from the Upper Permian and Lower Triassic of South Tibet and British Columbia:

- evidence for a diachronous mass extinction. *Palaios*, **18**, 153–167.
- Zeebe, R.E. and Westbroek, P., 2003. A simple model for the CaCO₃ saturation state of the ocean: the “Strangelove,” the “Neritan,” and the “Cretan” Ocean. *Geochem. Geophys. Geosyst.*, **4**, 1–26.
- Zhang, J., Quay, P.D. and Wilbur, D.O., 1995. Carbon-isotope fractionation during gas-water exchange and dissolution of CO₂. *Geochim. Cosmochim. Acta*, **59**, 107–114.
- Received 23 July 2003; revised version accepted 19 July 2005